

## Surface Adsorption and Transfer of Organomeraptans to Colloidal Gold and Direct Identification by Matrix Assisted Laser Desorption/Ionization Mass Spectrometry

John S. Kirk and Paul W. Bohn\*

Contribution from the Department of Chemistry and Beckman Institute for Advanced Science and Technology, University of Illinois at Urbana-Champaign, 600 South Mathews Avenue, Urbana, Illinois 61801

Received October 4, 2003; E-mail: bohn@scs.uiuc.edu

**Abstract:** The adsorption characteristics of two different organomeraptan adsorbates, 5-((2-(and-3)-S-(acetylmercapto)succinoyl)amino)fluorescein (SAMSA) and the peptide Cys-Lys-Trp-Ala-Lys-Trp-Ala-Trp (CKWAKWAK), on colloidal Au were studied, and the conjugates produced were characterized by UV–vis spectroscopy, transmission electron microscopy, and matrix-assisted laser desorption/ionization mass spectrometry (MALDI-MS). Fluorescence difference measurements of free thiols in solution were used to assemble surface adsorption isotherms on Au colloid revealing surface coverages of  $1.0 \times 10^{14}$  molecules  $\text{cm}^{-2}$  for SAMSA and  $3.1 \times 10^{14}$  molecules  $\text{cm}^{-2}$  for CKWAKWAK. The free energies of adsorption were calculated to be  $-48.4$  kJ/mol for SAMSA and  $-49.2$  kJ/mol for CKWAKWAK. UV–visible absorption spectroscopy and transmission electron microscopy reveal that the thiol/colloid conjugates flocculate under conditions where the net charge per colloid is small or neutral and that flocculated colloids can be resuspended by a change in pH to more basic for the acidic SAMSA/Au conjugates or to more acidic for the basic CKWAKWAK/Au conjugates. The reversible flocculation allows the conjugates to be readily separated from free adsorbate in solution and thereby prepared for further characterization. CKWAKWAK/colloid conjugates were analyzed by MALDI-MS, and the mass spectra show  $(M + H)^+$ ,  $(M + Na)^+$ , and  $(M + K)^+$  ions attributable to the peptide. The manipulations studied here constitute a powerful complement to microfluidic-based separation and analysis methods. Conjugating mass-limited analytes to Au colloids makes it possible to sequester and transfer small quantities of analytes with high efficiency.

### Introduction

Surface-modified Au colloids have drawn much attention recently for the vast potential they have as a new class of biomaterials, resulting from their interesting physical and chemical properties. The properties of the colloid can be tuned by changing the identity of a surface modifier appended to the colloid surface. They therefore lend themselves well to such applications as immunochemical tagging,<sup>1</sup> catalysis,<sup>2,3</sup> and chemical<sup>4,5</sup> and biochemical sensing.<sup>6,7</sup> A large amount of recent work has addressed the effects of adsorption of biomacromolecular conjugates at the colloid surface. For example, Helm and co-workers have studied the effect of surface-adsorbed biopolymers on the optical properties of gold colloids,<sup>8</sup> and Mirkin and co-workers have extensively investigated the detec-

tion of specific DNA sequences via DNA-linked colloid assemblies.<sup>6,9,10</sup> In these applications, the propensity of Au colloids to change their optical properties based on their size, shape, and state of aggregation is utilized to couple molecular binding at the surface of the colloid to a readout, e.g., color change.

One application not yet exploited is the use of colloids to capture and manipulate target species present in mass-limited samples. Mass-limited samples present a particularly important problem in contemporary sensing and chemical analysis, arising in arenas as diverse as the detection of virulent bioterror agents and the characterization of molecular trafficking in subcellular signaling processes.<sup>11,12</sup> Working with samples such as these, in which the target compounds may only be present in the zeptomole to attomole range, presents a panoply of challenges. Interfacial adsorption, in particular, is a vexing problem for mass-limited samples, inasmuch as the large surface areas encountered even in microfluidic structures and the irreversibility of many macromolecular adsorption phenomena can lead to

(1) Hayat, M. A. *Colloidal Gold: Principles, Methods, and Applications*; Academic Press: San Diego, 1989.

(2) Ingram, R. S.; Murray, R. W. *Langmuir* **1998**, *14*, 4115–4121.

(3) Li, H.; Luk, Y.-Y.; Mrksich, M. *Langmuir* **1999**, *15*, 4957–4959.

(4) Grabar, K. C.; Freeman, R. G.; Hommer, M. B.; Natan, M. J. *Anal. Chem.* **1995**, *67*, 735–743.

(5) Sun, Y.; Xia, Y. *Anal. Chem.* **2002**, *74*, 5297–5305.

(6) Elghanian, R.; Storhoff, J. J.; Mucic, R. C.; Letsinger, R. L.; Mirkin, C. A. *Science* **1997**, *277*, 1078–1080.

(7) Maxwell, D. J.; Taylor, J. R.; Nie, S. *J. Am. Chem. Soc.* **2002**, *124*, 9606–9612.

(8) Eck, D.; Helm, C. A.; Wagner, N. J.; Vaynberg, K. A. *Langmuir* **2001**, *17*, 957–960.

(9) Storhoff, J. J.; Elghanian, R.; Mucic, R. C.; Mirkin, C. A.; Letsinger, R. L. *J. Am. Chem. Soc.* **1998**, *120*, 1959–1964.

(10) Storhoff, J. J.; Lazarides, A. A.; Mucic, R. C.; Mirkin, C. A.; Letsinger, R. L.; Schatz, G. C. *J. Am. Chem. Soc.* **2000**, *122*, 4640–4650.

(11) Neiman, B.; Grushka, E.; Lev, O. *Anal. Chem.* **2001**, *73*, 5220–5227.

(12) Page, J. S.; Rubakhin, S. S.; Sweedler, J. V. *Anal. Chem.* **2002**, *74*, 497–503.

irreversible deletion of the target species from the fluid phase. One strategy that can be used to circumvent these problems is to arrange for the adsorption to occur on the surface of a carrier, which can subsequently be purposefully manipulated. For example, after being captured on the surface of colloidal Au, Lewis base-containing species can be manipulated, transported, and purified, all while maintaining the stability of the Au-adsorbate conjugates.<sup>13–15</sup> The colloid conjugates can subsequently be characterized by a number of analytical methods to identify the species bound to the surface of the colloid.<sup>16–18</sup>

This is of particular interest in transfer of material from microfluidic and nanofluidic devices, because the volumes and sample masses are typically quite small. The promise of microfluidic-based chemical instrumentation will be optimally realized when sequential chemical manipulations, e.g., separation, tagging, detection, identification, can be carried out within the microinstrument, in analogy with the complex sample workup protocols used for macroscopic samples. For instance, if the small amounts of sample from electrophoretic separations could be isolated and then transferred to characterization and identification instruments, it would greatly enhance the usefulness of microfluidic analysis.

Here, we detail a strategy for capturing and manipulating organomeraptans of varying molecular size on colloidal Au. The optimal use of this strategy is based on an understanding of the binding of organothiols to Au colloids, knowledge of the conditions under which the colloids may be aggregated, separated (centrifuged, filtered), and subsequently resuspended, and finally how the composition of the colloid adsorbates may be determined. The organomeraptans studied here represent a wide range of potential targets: from small molecules to larger biomolecules, such as peptides, from primarily acidic to predominantly basic compounds, and from synthetic to biologically derived targets. In addition to characterizing the Au-adsorbate chemistry for both small and intermediate molecular weight adsorbates, the mass spectrometric analysis of a peptide bound to the surface of gold colloids is reported using matrix assisted laser desorption/ionization time-of-flight (MALDI-TOF) mass spectrometry, a powerful method for identifying larger biological molecules that are potential targets.

## Experimental Section

**Materials.** The peptide, H<sub>2</sub>N-Cys-Lys-Trp-Ala-Lys-Trp-Ala-Trp-CO<sub>2</sub>NH<sub>2</sub> (CKWAKWAK) was synthesized and purified by the Protein Sciences Facility at the University of Illinois at Urbana-Champaign. The carboxy-terminus was amidated to ease synthesis as well as to eliminate the carboxylic acid, thereby shifting the pI of the peptide. 5-((2-(and-3)-S-(acetylmercapto)-succinoyl)amino)fluorescein (SAMSA) was purchased from Molecular Probes and was prepared by removal of the acetyl protecting group with NaOH prior to use. Colloids were purchased from British Biocell International and were sized to an average diameter of 23 nm by transmission electron microscopy (TEM).

**Conjugation.** SAMSA or CKWAKWAK was conjugated to colloidal Au by simple mixing of the thiol and gold colloid. SAMSA/colloid conjugation was typically carried out in 10mM borate, and CKWAKWAK/colloid conjugation was carried out in 15 μM tris(2-carboxyethyl)phosphine to optimize conditions for fluorescence characterization. The self-assembly of the thiol onto the gold colloid surface was allowed to proceed at room temperature for 1 h in the dark prior to any measurement or analysis.

**Adsorption Isotherm Measurements.** Excess thiol was separated from the conjugated thiol/colloid solutions by centrifugation at 11 000 g for 20 min using a Biofuge 17R centrifuge (Baxter Scientific). The supernatant solution was removed, without disturbing the colloid conjugate precipitate, and its fluorescence was measured using an SPEX Fluorolog-2 with a 450 W Xe lamp to determine the concentration of excess thiol. This concentration was used to calculate the amount of thiol adsorbed to the gold colloid by difference. Fluorescence measurements on SAMSA used an excitation wavelength of 491 nm and an emission wavelength of 513 nm. Measurements of CKWAKWAK used an excitation wavelength of 299 nm and an emission wavelength of 364 nm.

**Conjugate Characterization.** UV/visible absorption spectra were obtained using a Cary 3 UV–vis–NIR spectrophotometer. All spectra were taken with a spectral bandwidth of 1.5 nm at 0.5 nm data intervals and a signal averaging time of 0.1 s. To prepare samples for TEM characterization, SiO<sub>2</sub>-coated copper TEM grids obtained from Ted Pella, Inc. were placed on top of a small drop of colloid conjugate solution on Parafilm and allowed to sit for 30 min. The grids were removed, and excess solution was wicked away with filter paper. The samples were analyzed using a Philips CM200 transmission electron microscope operated at a 120 kV accelerating voltage.

**Matrix-Assisted Laser Desorption/Ionization Mass Spectrometry.** Samples were prepared by mixing 50 μL of 40 nM conjugate solution with 50 μL of acetone and then pipetting 1 μL spots onto a MALDI plate. A matrix of 40 mg/mL 2,5-dihydroxybenzoic acid (DHB) was prepared in 85% acetone, 15% water, and 0.3% trifluoroacetic acid. A 1 μL aliquot of the DHB matrix solution was pipetted onto the sample spots and allowed to dry. The samples were mass profiled using a Voyager DE STR time-of-flight mass spectrometer with delayed ion extraction (Applied Biosystems). Mass spectra were excited with an N<sub>2</sub> laser (337 nm) as the desorption/ionization source. The instrument was used in linear mode with an acceleration voltage of 20 kV and a delayed extraction of 350 ns. The grid voltage was set at 95%, and the guide wire voltage, at 0.1% of the acceleration voltage. The mass spectra acquired were the average of 200 laser shots. Prior to sample analysis, an external mass calibration was performed using a peptide standard containing an α-bag cell peptide, an acidic peptide, and bovine insulin, similar to mass calibration used by Page et al.<sup>12</sup>

## Results and Discussion

**SAMSA/Colloid Surface Adsorption Isotherm.** SAMSA is of interest as a model target because it is (a) acidic, (b) fluorescent, and (c) of small molecular weight. The first task in determining the utility of the Au colloid capture strategy for this target is to determine its adsorption isotherm on the colloid. Since the fluorescence of molecules close to metallic surfaces is strongly quenched,<sup>19,20</sup> the surface coverage of SAMSA must be determined indirectly through a difference measurement,

$$[S]_{\text{bound}} = [S]_0 - [S]_{\text{free}} \quad (1)$$

where  $[S]_0$  is the total concentration of SAMSA added originally,

- (13) Crumbliss, A. L.; Stonehuerner, J.; Henkens, R. W.; O'Daly, J. P.; Zhao, J. *New J. Chem.* **1994**, *18*, 327–339.
- (14) Novak, J. P.; Nickerson, C.; Franzen, S.; Feldheim, D. L. *Anal. Chem.* **2001**, *73*, 5758–5761.
- (15) de la Fuente, J. M.; Barrientos, A. G.; Rojas, T. C.; Rojo, J.; Canada, J.; Fernandez, A.; Penades, S. *Angew. Chem., Intl. Ed.* **2001**, *40*, 2258–2261.
- (16) Zhang, H.-L.; Evans, S. D.; Henderson, J. R.; Miles, R. E.; Shen, T. J. *Phys. Chem. B* **2003**, *107*, 6087–6095.
- (17) Kumar, A.; Mandal, S.; Selvakkannan, P. R.; Pasricha, R.; Mandale, A. B.; Sastry, M. *Langmuir* **2003**, *19*, 6277–6282.
- (18) Kim, H. S.; Lee, S. J.; Kim, N. H.; Yoon, J. K.; Park, H. K.; Kim, K. *Langmuir* **2003**, *19*, 6701–6710.

- (19) Lakowicz, J. R.; Shen, Y.; D'Auria, S.; Malicka, J.; Fang, J.; Gryczynski, Z.; Gryczynski, I. *Anal. Biochem.* **2002**, *301*, 261–277.
- (20) Templeton, A. C.; Cliffler, D. E.; Murray, R. W. *J. Am. Chem. Soc.* **1999**, *121*, 7081–7089.

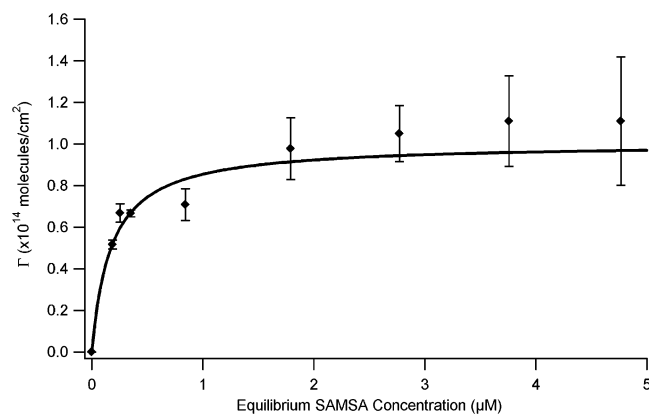


**Figure 1.** Plot of the number density of surface adsorbed SAMSA on 23 nm Au colloid as a function of equilibrium solution concentration, determined by difference fluorimetry. The solid line is a fit to a Langmuir isotherm, eq 3, and the error bars represent one standard deviation obtained from  $\geq 4$  replicate measurements.

$[S]_{\text{free}}$  is the concentration of free thiol in solution after conjugation, and  $[S]_{\text{bound}}$  is the bound thiol. The surface adsorbate density,  $\Gamma_{\text{bound}}$ , is calculated using the equilibrium bound SAMSA concentration after conjugation,  $[S]_{\text{bound}}$ , the concentration of colloid particles in solution,  $[N]_{\text{coll}}$ , and the average radius,  $r$ , of the colloid as determined by transmission electron microscopy, according to

$$\Gamma_{\text{bound}} = \frac{[S]_{\text{bound}}}{4\pi[N]_{\text{coll}}r^2} \quad (2)$$

Because the measurement is based on the difference between concentrations of SAMSA before and after conjugation, this difference must be significant to minimize experimental error. The concentration difference is controlled by two factors: the concentration of colloid in and the total volume of the conjugation solution. Larger amounts of colloid in solution result in larger amounts of SAMSA adsorbed from solution and, thus, a larger difference in fluorescence intensity before and after conjugation. Clearly smaller volumes also lead to larger differences in SAMSA concentration for the same mass adsorbed from solution. Thus, to account properly for the arbitrary number of colloidal particles in solution and the total solution volume when building the adsorption isotherms, the surface coverage,  $\Gamma_{\text{bound}}$ , is plotted vs the equilibrium concentration of thiol after conjugation,  $[S]_{\text{free}}$ .

Figure 1 shows the accumulated surface coverages,  $\Gamma_{\text{bound}}$ , for different equilibrium bulk solution concentrations of SAMSA. Saturation of  $\Gamma_{\text{bound}}$  is observed at equilibrium concentrations  $[S]_{\text{free}} \geq 2 \mu\text{M}$ . The data shown in Figure 1 are well-fit by a Langmuir adsorption isotherm,

$$\Gamma = \frac{\Gamma_{\text{max}} K_L [S]_{\text{free}}}{1 + K_L [S]_{\text{free}}} \quad (3)$$

where  $\Gamma_{\text{max}}$  is the maximum coverage and  $K_L$  is a constant representing the inverse of the bulk solution concentration of adsorbate required to reach half of the maximum surface coverage.<sup>21</sup> Fitting was weighted with the standard deviation of replicate measurements for each data point. The fit of the

data in Figure 1 to eq 3 yields  $\Gamma_{\text{max}} = (1.0 \pm 0.1) \times 10^{14}$  molecules  $\text{cm}^{-2}$  and  $K_L = (5.8 \pm 1.1) \times 10^6 \text{ M}^{-1}$ .

The free energy of adsorption,  $\Delta G_{\text{ads}}$ , can be obtained from  $K_L$  through the relationship,

$$\Delta G_{\text{ads}} = -RT \ln \frac{K_L}{V_m} \quad (4)$$

where  $R$  is the gas constant,  $T$  is the temperature (297 K), and  $V_m$  is the molar volume of the solution.<sup>21</sup> Because the SAMSA concentrations used are small, the molar volume of water,  $18.0 \times 10^{-3} \text{ M}^{-1}$ , can be used for  $V_m$ . From eq 4, the free energy of adsorption of SAMSA to gold colloid is  $-48.4 \pm 0.5 \text{ kJ/mol}$ .

This measurement for the adsorption of the small molecule adsorbate SAMSA may be compared to adsorption free energies for alkanethiols. For example, Karpovich and Blanchard report  $\Delta G_{\text{ads}} = -22.3 \text{ kJ/mol}$  for adsorption of 1-octadecanethiol from cyclohexane onto a planar microcrystalline gold surface.<sup>22</sup> The adsorption free energy contains a contribution from the solvation energy of the adsorbate, and this is likely responsible at least in part for the enhanced  $\Delta G_{\text{ads}}$  for SAMSA from  $\text{H}_2\text{O}$ . As an example of macromolecular adsorption, Yang and co-workers found that thiol-derivatized 718 base pair double-stranded DNA adsorbed from aqueous solution onto a planar gold surface with  $\Delta G_{\text{ads}} = -35.1 \text{ kJ/mol}$ .<sup>23</sup> Of course, as a polyelectrolyte, the adsorption of DNA is intimately tied to the ionic strength of the adsorbing solution, and intermolecular Coulomb repulsion plays a large role in determining  $\Delta G_{\text{ads}}$ . The difficulties in interpreting measurements of  $\Delta G_{\text{ads}}$  and sticking probabilities from kinetic data have been thoroughly discussed by Jung and Campbell in the context of the adsorption of alkanethiols of varying chain length from ethanol onto planar Au.<sup>24</sup> The principal point here is that the  $\Delta G_{\text{ads}}$  measured from the isotherm for SAMSA adsorption onto Au is comparable to results for organomeraptan adsorption onto planar Au. The  $\Delta G_{\text{ads}}$  values would not necessarily be expected to agree with those for the more commonly encountered alkanethiols on planar Au, given differences between (1) the initial surface chemistry presented by stabilized Au colloids and that of planar Au films, (2) solvents (aqueous buffer vs ethanol or hexane), and (3) the packing of a saturated layer of the aromatic SAMSA on a spherical particle vs the well-ordered packing of alkanethiols on planar Au.<sup>25–28</sup> The other important point regarding the isotherm is that it establishes the solution conditions, i.e.,  $[S]_{\text{free}} > 2 \mu\text{M}$ , under which it is possible to achieve saturation coverage on the Au colloid.

**SAMSA/Colloid UV–visible Absorption.** The underivatized colloid in solution is red, and this color does not change after conjugation of the colloid with SAMSA. The UV–visible absorption spectrum of a SAMSA/colloid conjugate assembled from a solution containing 320 pM Au colloid and 10  $\mu\text{M}$  SAMSA is shown in Figure 2 and is very similar to that of bare gold colloid (not shown). SAMSA/colloid conjugates are susceptible to flocculation from changes in pH as is evident

- (22) Karpovich, D. S.; Blanchard, G. J. *Langmuir* **1994**, *10*, 3315–3322.  
 (23) Yang, M.; Yau, H. C. M.; Chan, H. L. *Langmuir* **1998**, *14*, 6121–6129.  
 (24) Jung, L. S.; Campbell, C. T. *J. Phys. Chem. B* **2000**, *104*, 11168–11178.  
 (25) Camillone, N., III; Chidsey, C.; Liu, G. Y.; Putvinski, T.; Scoles, G. *J. Chem. Phys.* **1991**, *94*, 8493.  
 (26) Fenter, P.; Eisenberger, P.; Li, J.; Camillone, N.; Bernasek, S.; Scoles, G.; Ramanarayanan, T. A.; Liang, K. S. *Langmuir* **1991**, *7*, 2013.  
 (27) Poirier, G. E.; Tarlov, M. J. *Langmuir* **1994**, *10*, 2853–2856.  
 (28) Poirier, G.; Pylant, E. *Science* **1996**, *272*, 1145.

(21) Lyklema, J.; Leeuwen, H. P. van. *Fundamentals of Interface and Colloid Science*; Academic Press: San Diego, CA, 1991.

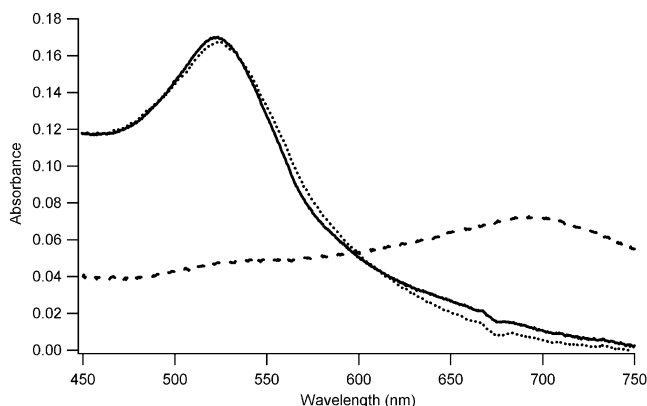


**Figure 2.** UV-visible absorption spectra of 320 pM SAMSA/colloid conjugates under various pH conditions: (—) in 0.5 mM borate, pH 8; (---) with 2 mM HCl added, pH 2; and (···) with 4 mM NaOH added, pH 10.

from Figure 2. When the conjugate is formed in the presence of HCl (pH = 2), the characteristic strong absorbance at 522 nm decreases significantly, and a broad feature to the low energy side, characteristic of multi-colloid aggregates, appears. These spectral changes, thus, indicate flocculation of the conjugates in acidic media.<sup>10,29</sup> Furthermore, because there is little remaining absorption at 522 nm, it is likely that the preponderance of colloids are tied up in aggregates, with little unaggregated population remaining.

When NaOH is added to these conjugates flocculated with HCl in sufficient amount to shift the solution basic (pH = 10), the spectral changes observed upon acidification are reversed. The red-shifted feature at ~700 nm disappears, and the strong absorbance at ca. 522 nm returns. This reversible behavior upon sequential exposure to acid, then base, is consistent with the presence of the carboxylic acid-containing SAMSA at the Au colloid surface inferred in the surface adsorption measurements. The reversion of the colloid conjugate spectrum to the original unflocculated state upon treatment with base, and subsequent deprotonation of the carboxylic acid surface moieties, indicates that the dispersion of these colloids in solution can be controlled, at least in part, by the surface charge density.

It is well-documented that changes in solution conditions, such as temperature and pH, can cause flocculation in colloid conjugates.<sup>29</sup> Flocculation caused by such environmental changes is not always reversible. While reversible flocculation of Au colloids has been shown in some systems to be controllable by temperature changes,<sup>30</sup> coordination chemistry,<sup>31</sup> and lectin chemistry,<sup>32</sup> reports of pH-reversible aggregation are rare.<sup>33</sup> For example, Sastry and co-workers observed that while flocculation of modified Ag colloids derivatized with *p*-carboxythiophenol is semireversible,<sup>34</sup> Au colloids modified with the same thiol do not flocculate reversibly upon changing pH.<sup>35</sup>

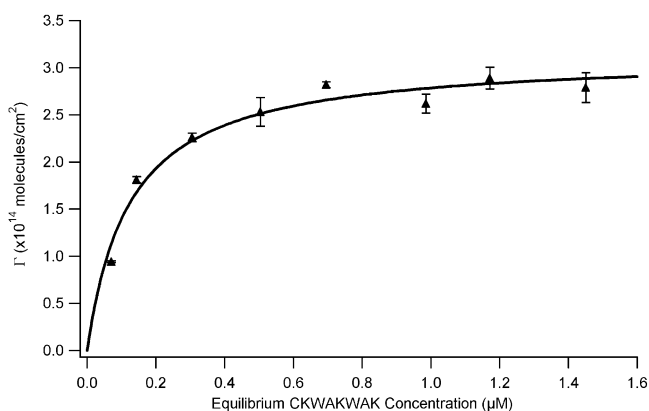


**Figure 3.** Plot of the number density of surface adsorbed CKWAKWAK on 23 nm Au colloid as a function of equilibrium solution concentration, determined by difference fluorimetry. The solid line is a fit to a Langmuir isotherm, eq 3, and the error bars represent one standard deviation obtained from four replicate measurements.

In the conjugate experiments, the ease with which the colloid conjugate could be resuspended after centrifugation was strongly correlated with the state of flocculation prior to centrifugation. Conjugates that were dispersed, i.e., red in color, were easily resuspended with the simple shaking of the centrifuge tube. Flocculated, i.e., purplish-gray, colloid adhered to the walls of the centrifuge tube after centrifugation and was not resuspended, even after extended sonication. Hence, the initial flocculation state of the colloid conjugates was important to the success of using centrifugation to purify the conjugates for MALDI mass spectrometry.

**CKWAKWAK/Colloid Surface Adsorption Isotherm.** The adsorption of CKWAKWAK onto colloidal Au was measured using the fluorescence difference measurement protocol described above. Figure 3 shows the isotherm for adsorption of CKWAKWAK onto colloidal Au at various equilibrium concentrations of CKWAKWAK,  $[S]_{\text{free}}$ . The surface coverage of CKWAKWAK reaches a saturation coverage beyond an equilibrium concentration,  $[\text{CKWAKWAK}] = 0.5 \mu\text{M}$ , a factor of 4 lower concentration than that of SAMSA. Fitting the adsorption data to a Langmuir adsorption isotherm, shown in Figure 3, yields  $\Gamma_{\text{max}} = (3.1 \pm 0.1) \times 10^{14}$  molecules  $\text{cm}^{-2}$  and  $K_L = (8.0 \pm 1.2) \times 10^6 \text{ M}^{-1}$ . The free energy of adsorption for CKWAKWAK obtained from eq 4 gives  $\Delta G_{\text{ads}} = -49.2 \pm 0.4$  kJ/mol, similar to the adsorption energy of  $-48.4$  kJ/mol obtained for SAMSA on Au colloid. The behavior of CKWAKWAK indicates that it is a reasonably surface active molecule, certainly more surface active from aqueous solution than SAMSA. Stringent precautions were taken to guard against multilayer formation which would skew the saturation coverage to larger apparent values. Despite this, the saturation surface coverage,  $\Gamma_{\text{max}}$ , is somewhat larger than expected. Part of the surface coverage may be due to the physisorption of the peptide to the colloid. However, control experiments, in which 1% SDS was utilized to block physisorption, yielded the same coverages within experimental error. Ultimately, the utility of the Au colloid-carrier strategy depends on being able to capture macromolecular targets efficiently, and the isotherm data indicate that the Au-CKWAKWAK conjugates satisfy this criterion.

**CKWAKWAK/Colloid UV-visible Absorption.** When CKWAKWAK is conjugated to bare Au colloid, the initial red

(29) Weisbecker, C. S.; Merritt, M. V.; Whitesides, G. M. *Langmuir* **1996**, *12*, 3763–3772.

(30) Nath, N.; Chilkoti, A. J. *Am. Chem. Soc.* **2001**, *123*, 8197–8202.

(31) Templeton, A. C.; Zamborini, F. P.; Wuelfing, W. P.; Murray, R. W. *Langmuir* **2000**, *16*, 6682–6688.

(32) Otsuka, H.; Akiyama, Y.; Kataoka, K. *J. Am. Chem. Soc.* **2001**, *123*, 8226–8230.

(33) Li, G.; Lauer, M.; Schulz, A.; Boettcher, C.; Li, F.; Fuhrhop, J.-H. *Langmuir* **2003**, *19*, 6483–6491.

(34) Sastry, M.; Mayya, K. S.; Bandyopadhyay, K. *Colloids Surf., A* **1997**, *127*, 221–228.

(35) Mayya, K. S.; Patil, V.; Sastry, M. *Langmuir* **1997**, *13*, 3944–3947.

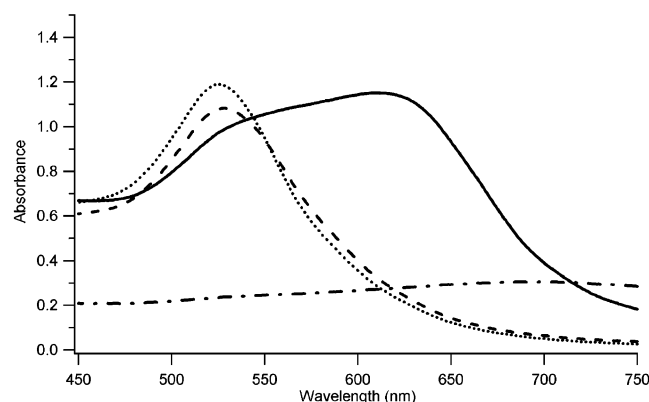


**Figure 4.** UV-visible absorption spectra of 2 nM CKWAKWAK/colloid conjugates under different conditions: (—) unbuffered (pH 5), (---) in 1 mM NaOH (pH 9), (···) in 1 mM HCl (pH 2), and (- · - ·) colloid conjugates from the pH 9 solution centrifuged, decanted, and then resuspended in 1 mM HCl solution (pH 2).

solution color changes to purple. This color is illustrated by the absorption spectrum of a 2 nM colloid solution conjugated with 20  $\mu$ M CKWAKWAK shown in Figure 4. The unbuffered CKWAKWAK/colloid conjugate exhibits unresolved absorption maxima at ca. 530 and 620 nm, while the acidified conjugate displayed a single well-resolved absorption maximum at 525 nm. This suggests that in unbuffered solution the colloid is present in a state of intermediate flocculation with a significant population still present as dispersed individual particles and that the pH-controlled charge state of the adsorbate plays a deciding role in determining the state of aggregation. The addition of 1 mM NaOH to the unbuffered conjugate solution removes the large spectral features, resulting in a spectrum with no discernible features, characteristic of flocculated colloid. However, when this basic solution is centrifuged and decanted and 1 mM HCl is added, the large absorption peak reappears at 528 nm, indicating dispersion of the colloid conjugate.

A crucial feature of any strategy for manipulating mass-limited samples is the ability to physically isolate the target compound and to transfer it quantitatively. Certainly the ability to bind, separate, and then resuspend the Au-CKWAKWAK colloid conjugates satisfies this demand. Thus, these observations open the door for the use of Au colloids as carriers with which to manipulate small quantities of peptides, especially for those peptides that contain significant numbers of ionizable moieties whose charge state can be controlled to direct flocculation.

**CKWAKWAK/Colloid Transmission Electron Microscopy.** The optical absorption spectra presented in Figure 4 strongly suggest that Au-CKWAKWAK colloid conjugates in acidic media are dominated by well-separated single particles. To address the aggregation state definitively, electron micrographs of CKWAKWAK/colloid conjugates produced under various conditions were obtained and are shown in Figure 5. Also shown with each TEM micrograph is the corresponding histogram of measured nearest neighbor distances between colloidal particles. Electron micrographs of dry colloid on the surface of a TEM grid are not completely accurate representations of the inter-colloid spacing in solution, since flocculation may occur as the solvent evaporates. However, the electron micrographs should present a lower limit on the solution interparticle spacing, since flocculated colloid would not be

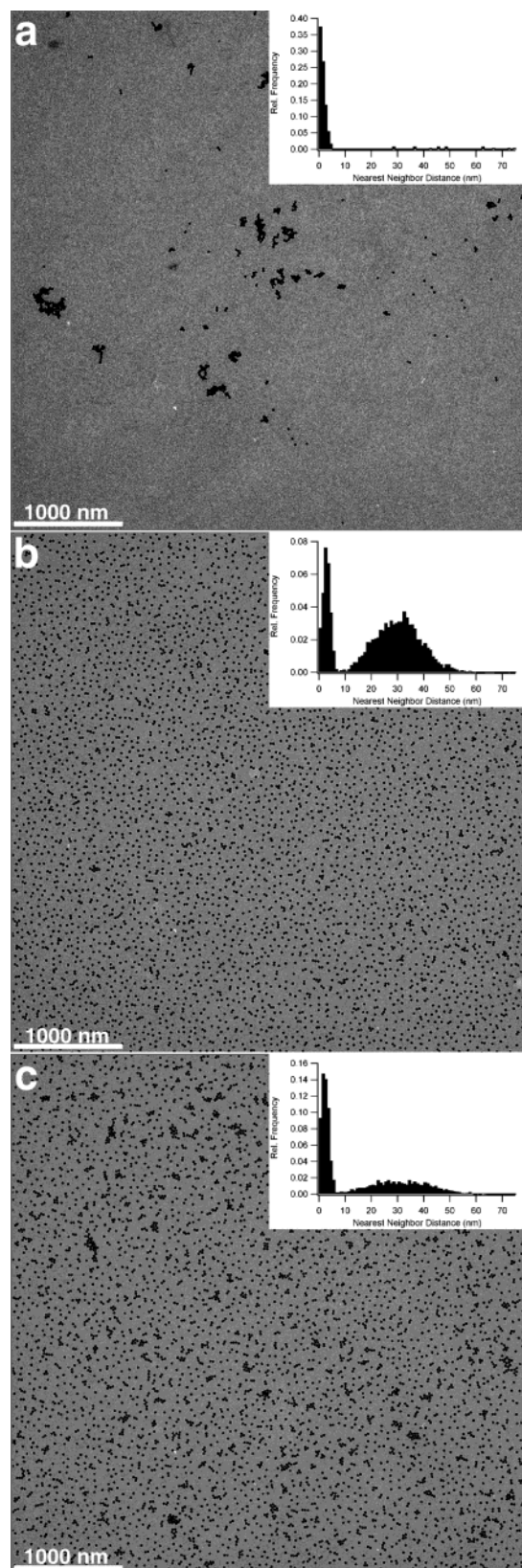


**Figure 5.** Transmission electron micrographs and nearest neighbor distance histograms of (a) unbuffered CKWAKWAK/colloid conjugates, (b) CKWAKWAK/colloid conjugates in 1 mM HCl, and (c) CKWAKWAK/colloid conjugates prepared initially in 1 mM NaOH and then centrifuged, decanted, and resuspended in 1 mM HCl.

expected to disperse upon solvent evaporation. Thus, TEM micrographs showing highly dispersed colloids on the surface

of the TEM grid can be interpreted to result from highly dispersed colloids in solution.

Figure 5a shows the unbuffered CKWAKWAK/colloid conjugate. Single colloids, as well as clusters of colloids, are present in the image. The presence of single colloids in addition to small clusters of flocculated colloid is consistent with the observation of two peaks in the UV-visible absorption spectrum of this solution. The presence of single colloids can explain the existence of the significant absorption at  $\sim 530$  nm, a feature characteristic of dispersed colloid, while the presence of flocculated colloid is likely responsible for the red-shifted absorption feature near  $\sim 630$  nm, since absorption in this red-shifted region has been assigned to chains of flocculated colloids.<sup>36</sup> The presence of both absorption features is also seen in the spectra of Au nanorods, where the two absorption features are attributed to the orthogonal resonances of surface plasmons of the Au along the short and long axes of the nanorod.<sup>37</sup> The short and long axes would correspond here to individual and aggregated colloids, respectively.

The micrograph in Figure 5b shows CKWAKWAK/colloid conjugate deposited from 1 mM HCl solution. Most of the colloids present in the image are single colloids, with only a small fraction of the colloids present in clusters. The histogram of interparticle distances shows that the majority of the population is present in the single particle band with a mean interparticle spacing,  $\bar{d} = 32$  nm. Because the settling of colloids onto the surface of the TEM grid is controlled by the same repulsive electrostatic forces that keep the conjugates dispersed when in solution and because solvent evaporation is expected to increase the state of flocculation, these data confirm that the colloid conjugates in acidic solution are well-separated. The straightforward interpretation is that at low pH the large fraction of protonated amines produces a large net positive charge on the nanoparticles, which results in a well-dispersed collection of particles.

Figure 5c shows a CKWAKWAK/colloid conjugate which was initially flocculated in basic solution (1 mM NaOH), then separated from that solution and resuspended in 1 mM HCl. Both individual colloids and small clusters are present. Interestingly the interparticle spacing in the single particle band is very close to the value for the colloids deposited from acidic media, shown in Figure 5b, although the width of the single particle band is slightly larger in Figure 5c. This is significantly different than TEM micrographs of conjugates in 1 mM NaOH, which only exhibit clusters of conjugates (images not shown). The conjugates in Figure 5c have evidently been redispersed, at least partially, by the change to lower pH. However, a small number of clusters remain, as signified by the relative magnitude of the small spacing peak in the histogram of Figure 5, compared to Figure 5b. Such clusters may result, either because they were not redispersed completely by the charging of the conjugate surfaces, or they may simply have flocculated as the concentration of the conjugates increased during solvent evaporation. In either case the dominant behavior, consistent with the absorption spectra, is redispersion of flocculated CKWAKWAK/Au colloids, upon lowering the pH. Furthermore, the interparticle distance histograms of Figure 5b and c are similar, suggesting

that the same repulsive forces are present between individual colloids in both acidic solutions.

The TEM micrographs allow the absorption spectra of Figure 4 to be interpreted in a more subtle way. Because the absorption spectrum for flocculated colloids results in a broad featureless low-intensity absorption, the absorption spectra can be interpreted to result principally from the dispersed fraction of the colloid population. Thus, the presence of a single band at 525 nm for the CKWAKWAK-Au colloid conjugate in acidic solution is indicative of a solution in which single well-dispersed colloidal particles are the dominant, not the sole, feature.

**CKWAKWAK/Colloid MALDI-MS.** To prepare CKWAKWAK/colloid conjugate for MALDI-MS, the assembled conjugate solution was purified from excess CKWAKWAK by centrifuging, decanting, and resuspending multiple times. Each centrifuge-decant-resuspend cycle dilutes the excess CKWAKWAK solution by a factor of 20. Because the peptide target is selectively bound to the Au colloid, other impurities in the sample, e.g., salts and other matrix interferences, can be effectively removed by centrifugation followed by decanting the supernatant. This procedure is similar, in the ease of purification and handling of low-level analytes, to the work done by Caprioli<sup>38</sup> and Tomer<sup>39</sup> with chromatographic beads. In the Au conjugate work here, however, the analyte is directly bound to the colloid and is not removed prior to MALDI analysis of the conjugate.

Each conjugate solution was cycled 7 times so that the free solution concentration of CKWAKWAK, which was originally 20  $\mu\text{M}$  (preconjugation), was estimated to be present at less than 16 fM in the solution used to prepare the MALDI samples. Control experiments were performed on (1) MALDI samples prepared from colloid without CKWAKWAK and (2) samples of CKWAKWAK without colloid that had undergone the same number of centrifuge-decant-resuspend cycles. Neither control sample showed any mass spectral peaks above the background in the molecular ion region. Control experiment 1 indicates that the mass spectral peaks observed in the range  $1019 \leq m/z \leq 1058$  are authentic CKWAKWAK peaks, and control experiment 2 shows that nonadsorbed CKWAKWAK is removed to levels below the MALDI detection limit by the centrifuge-decant-resuspend cycles.

Approximately  $6 \times 10^{-17}$  mol of Au-CKWAKWAK/colloid conjugate particles was sampled per spot. Since the surface adsorption measurements put the average CKWAKWAK loading at  $\sim 4500$  molecules/colloid, the number of CKWAKWAK molecules sampled is estimated at  $3 \times 10^{-13}$  mol of CKWAKWAK. A typical MALDI-MS of CKWAKWAK/colloid conjugate is shown in Figure 6. The molecular weight of CKWAKWAK is 1018.5 Da; thus the peak at  $m/z$  of 1019.8 is assigned as  $(M + H)^+$ , and the peaks at 1041.7 and 1057.5  $m/z$ , being  $\sim 23$  and 39 Da larger than the molecular weight, are assigned to  $(M + Na)^+$  and  $(M + K)^+$ , respectively. The mass spectral signal was observed after a series of serial dilutions, such that the estimated mass sampled was  $9 \times 10^{-15}$  mol of CKWAKWAK.

There have been numerous attempts to characterize thiol/colloid conjugates by mass spectrometry with mixed results.

(36) Lazarides, A. A.; Schatz, G. C. *J. Phys. Chem. B* **2000**, *104*, 460-467.  
(37) Yu, Y.-Y.; Chang, S.-S.; Lee, C.-L.; Wang, C. R. C. *J. Phys. Chem. B* **1997**, *101*, 6661-6664.

(38) Zhang, H.; Andren, P. E.; Caprioli, R. M. *J. Mass Spectrom.* **1995**, *30*, 1768-1771.  
(39) Papac, D. I.; Hoyes, J.; Tomer, K. B. *Anal. Chem.* **1994**, *66*, 2609-2613.

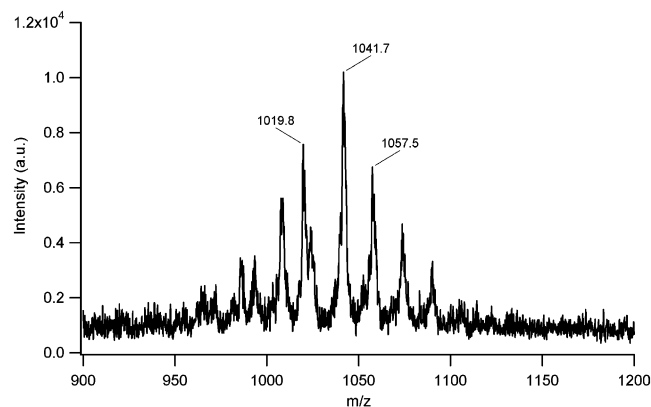


**Figure 6.** Expanded molecular ion region of the MALDI mass spectrum of CKWAKWAK/colloid conjugate prepared in 20 mg/mL 2,5-dihydroxybenzoic acid.

Direct routes to molecular identification by laser desorption result either in the detection of the entire colloid conjugate<sup>40–42</sup> or in the cleavage of the C–S bond.<sup>42–45</sup> Thermal desorption has been used to prepare ions from colloid conjugates for mass spectrometry;<sup>46,47</sup> however, this method is limited to smaller alkanethiols that are readily thermally desorbed and is not relevant to larger biomolecules. Inductively coupled plasma sources have been used for analyzing conjugates,<sup>48,49</sup> but this method is destructive of the entire conjugate and therefore eliminates the prospect of positively identifying the ligands. Jordan and co-workers have used MALDI to characterize polymerization at the surface of gold colloids by etching the gold core with NaCN.<sup>50</sup> However, the etching step requires 16 h to complete followed by an organic phase extraction of the ligand. In contrast, definitive molecular ion information is obtained from the Au–CKWAKWAK conjugates by the simple

expedient of mixing a buffered colloid solution with adsorbate under pH conditions designed to keep the colloidal particles charged, and thus well-dispersed. Clearly optimization of the physical isolation process can be expected to enhance the yield of single nanoparticles and, thereby, improve the limit of detection of peptide, pushing peptide identification to the levels needed for mass-limited samples.

## Conclusions

Characterization of mass-limited samples is a challenging problem that lies ahead of progress on questions as diverse as understanding subcellular signal trafficking to identification of biothreat agents. To bring the full armamentarium of modern chemical analysis to bear on these issues, it is necessary to develop protocols for handling these samples in such a way that they can be transferred between instruments and manipulative experiments without loss. The results presented here address the possibility of exploiting Au-thiol chemistry, through agency of Au-colloid conjugates, to accomplish these transfers and manipulations. The first requirement of such a strategy is that the Au colloids be capable of efficient capture of the target species. The surface adsorption isotherms for the SAMSA and CKWAKWAK Au colloid conjugates demonstrate the efficient capture by Au colloids in the range of 1  $\mu$ M for these two adsorbates. UV–visible absorption spectroscopy and TEM microscopy have been used to identify how these conjugates can be manipulated, through changes in pH, to systematically purify and concentrate colloid conjugates. The proof-of-principle experiments were carried out with a small molecular weight acidic adsorbate and an intermediate molecular weight basic adsorbate, so there is reason to believe that the approach may be general for adsorbates containing Brønsted acid/base functionalities. Finally, a key requirement for the ultimate use of such a carrier strategy is the ability to identify the adsorbates being carried by the colloid conjugates. MALDI-MS was used to acquire definitive identification of the CKWAKWAK biomolecule directly from the surface of an Au colloid. An intact  $(M + H)^+$  ion, in addition to  $(M + Na)^+$  and  $(M + K)^+$  ions, positively identifies the adsorbate molecule on the surface of the Au colloid. As a whole, these results demonstrate the potential for Au colloids to be an effective solution to the problems of the capture and manipulation of mass-limited target species.

**Acknowledgment.** Financial support from the U.S. Department of Energy (DEFG02-88ER13949) is gratefully acknowledged. We thank D. Weber for help generating the histograms for the TEM images, J.V. Sweedler for use of the MALDI instrument, and Q. Wang for assistance in acquiring MALDI mass spectra.

JA030573M

- (40) Schaaff, T. G.; Shafiqullin, M. N.; Khoury, J. T.; Vezmar, I.; Whetten, R. L.; Cullen, W. G.; First, P. N.; Wing, C.; Ascencio, J.; Yacaman, M. J. *J. Phys. Chem. B* **1997**, *101*, 7885–7891.
- (41) Alvarez, M. M.; Khoury, J. T.; Schaaff, T. G.; Shafiqullin, M.; Vezmar, I.; Whetten, R. L. *Chem. Phys. Lett.* **1997**, *266*, 91–98.
- (42) Hicks, J. F.; Templeton, A. C.; Chen, S.; Sheran, K. M.; Jasti, R.; Murray, R. W.; Debord, J.; Schaaff, T. G.; Whetten, R. L. *Anal. Chem.* **1999**, *71*, 3703–3711.
- (43) Schaaff, T. G.; Shafiqullin, M. N.; Khoury, J. T.; Vezmar, I.; Whetten, R. L. *J. Phys. Chem. B* **2001**, *105*, 8785–8796.
- (44) Negishi, Y.; Tsukuda, T. *J. Am. Chem. Soc.* **2003**, *125*, 4046–4047.
- (45) Arnold, R. J.; Reilly, J. P. *J. Am. Chem. Soc.* **1998**, *120*, 1528–1532.
- (46) Sandhyarani, N.; Resmi, M. R.; Unnikrishnan, R.; Vidyasagar, K.; Ma, S.; Antony, M. P.; Selvam, G. P.; Visalakshi, V.; Chandrakumar, N.; Pandian, K.; Tao, Y.-T.; Pradeep, T. *Chem. Mater.* **2000**, *12*, 104–113.
- (47) Hostetler, M. J.; Wingate, J. E.; Zhong, C.-J.; Harris, J. E.; Vachet, R. W.; Clark, M. R.; Londono, J. D.; Green, S. J.; Stokes, J. J.; Wignall, G. D.; Glush, G. L.; Porter, M. D.; Evans, N. D.; Murray, R. W. *Langmuir* **1998**, *14*, 17–30.
- (48) Andreu, E. J.; De Llano, J. J. M.; Moreno, I.; Knecht, E. *J. Histochem. Cytochem.* **1998**, *46*, 1199–1201.
- (49) Martin de Llano, J. J.; Andreu, E. J.; Knecht, E. *Anal. Biochem.* **1996**, *243*, 210–217.
- (50) Jordan, R.; West, N.; Ulman, A.; Chou, Y.-M.; Nuyken, O. *Macromolecules* **2001**, *34*, 1606–1611.